ASTRONOMY & ASTROPHYSICS
SUPPLEMENT SERIES

Astron. Astrophys. Suppl. Ser. **142**, 347–352 (2000)

The stellar content and distance to the nearby blue compact dwarf galaxy NGC 6789⋆

I. Drozdovsky[1] **and N. Tikhonov**[2]

[1] Astronomical Institute, St.-Petersburg State University, Petrodvoretz 198904, Russia
[2] Special Astrophysical Observatory, N.Arkhyz, Karachai-Circassian Rep. 357147, Russia

Received August 21, 1998; accepted October 19, 1999

Abstract. In this paper we present the results of a detailed B, V, R, I, and Hα study of the isolated nearby blue compact dwarf (BCD) galaxy NGC 6789. The observed galaxy has not yet been resolved into stars up to now. On CCD frames obtained with 6 m BTA telescope and 2.5 m Nordic telescope the galaxy is well resolved. Its colour-magnitude diagram confirms the two component (core-halo) galaxy morphology, which consists of two stellar populations distinct in structure and colour: an inner high surface-brightness young population within 150 pc from the center of the galaxy, and a relatively low surface-brightness intermediate-age population extending out to at least 600 pc. The distance to the galaxy, estimated from the tip of the red giant branch (TRGB) is 2.1 Mpc which places NGC 6789 close to the Local Group. From the mean colour of the RGB, the mean metal abundance of the halo population is estimated as [Fe/H] $\simeq -1$ dex.

Key words: nearby galaxies: dwarf galaxies (NGC 6789): distance moduli: star content

1. Introduction

In spite of its New General Catalog membership this galaxy is poor studied.

NGC 6789 is in the list of 260 new Local Volume galaxies by Karachentseva & Karachentsev (1998), who used the POSS-II and ESO-SERC survey. The NGC 6789 galaxy is outstanding by its high surface brightness in central region, small radial velocity ($V_0 = -157$ km s^{-1} Huchra 1995), and spatial isolation. But, in spite of its optical high surface brightness, it was undetected in H I with the Effelsberg 100 m radiotelescope (Huchtmeier et al. 1997).

We resolved this galaxy into stars with the 6 m telescope in April 1996 under rather poor seeing conditions. In a July 1996 run with the 6 m telescope we have constructed a CM diagram of the NGC 6789, which shows the existence of two distinct groups of stellar population placed within different radii from galaxy optical center. The photometric limit in the red frames did not allow to locate the RGB.

Later optical spectral observations with the 6 m-telescope long slit spectrometer UAGS revealed H II gas in NGC 6789 (Karachentsev & Makarov 1998). The Hα radial velocity is -141 ± 8 km s^{-1}, close to value of Huchra (1995).

Deep photometric observations with Nordic 2.5 m telescope with better seeing revealed the RGB, while Hα frames have shown large H II regions in the central region and 3 compact objects in the outer region.

Section 2 briefly presents the observations. In Sect. 3 we present the results of our work: in Sect. 3.1 an overview of the CM diagram is given and used to estimate the distance to NGC 6789 (Sect. 3.3) and its metallicity (Sect. 3.2). In Sect. 3.4 the distribution of surface brightness is discussed. Finally, the results are summarized in Sect. 4.

2. Observations and reductions

The observations of NGC 6789 were made in 1996 and 1997 at the prime focus of the 6 m telescope, at the Cassegrain focus of the 1 m telescope of SAO (Russia) with standard Johnson B, V and Cousins R_c, I_c filters, and also at the Nordic 2.5-meter telescope (NOT) with the HiRAC instrument in the V, I_c, and Hα bands. At the 6 m telescope we used a ISD017A CCD detector with 1050×1170 pixels, each 16×16 μm ($0\farcs137 \times 0\farcs137$), at the 1 m telescope we had a K983 CCD detector with 530 ×

Send offprint requests to: I. Drozdovsky;
e-mail: dio@astro.spbu.ru

⋆ Data available in electronic form at the CDS via anonymous ftp to cdsarc.u-strasbg.fr or via http://cdsweb.u-strasbg.fr/Abstract.html

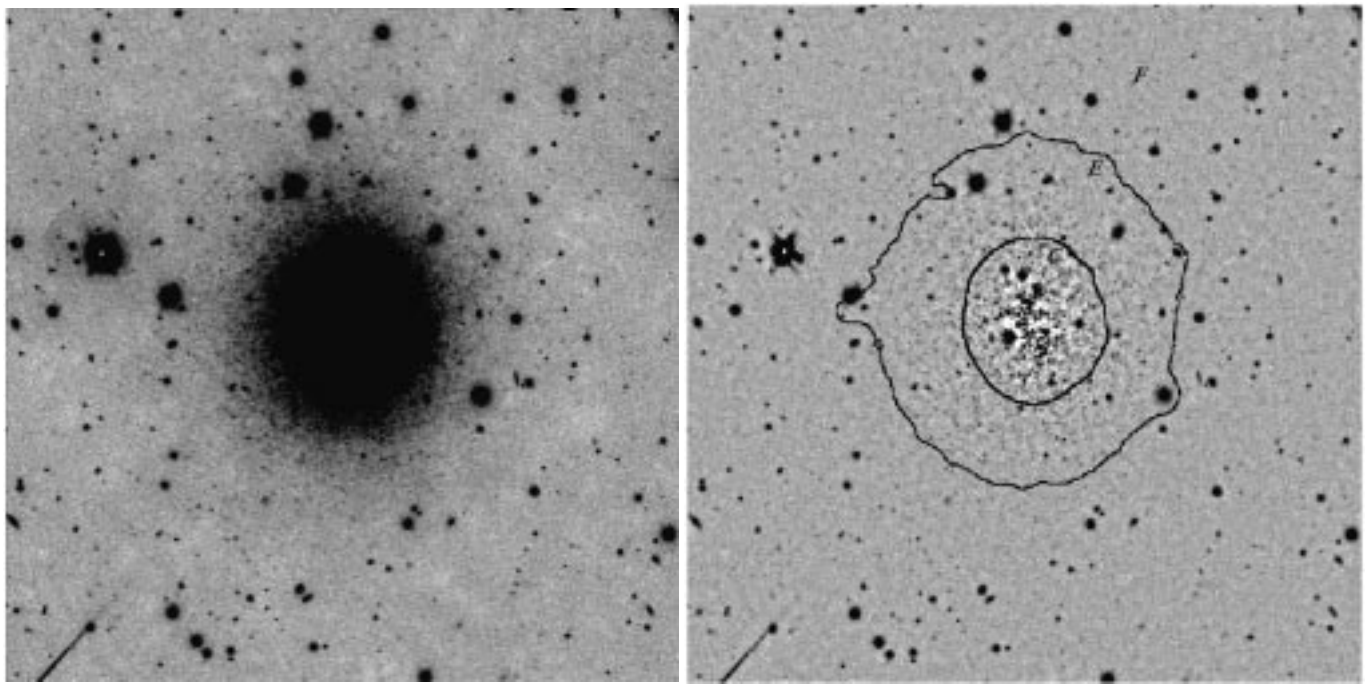

Fig. 1. NGC 6789 in the I band. **a)** The original frame, **b)** the same part after subtracting the median, smoothed with a window of $10 \times (FWHM)$. The size of the CCD frame is 3.7 by 3.7 arcmin. North left, East top. The isophotes correspond to 22.5 mag/$\Box''$ and 24.2 mag/$\Box''$. They are used to define the central region (C), the perefery (E) and the foreground stars (F)

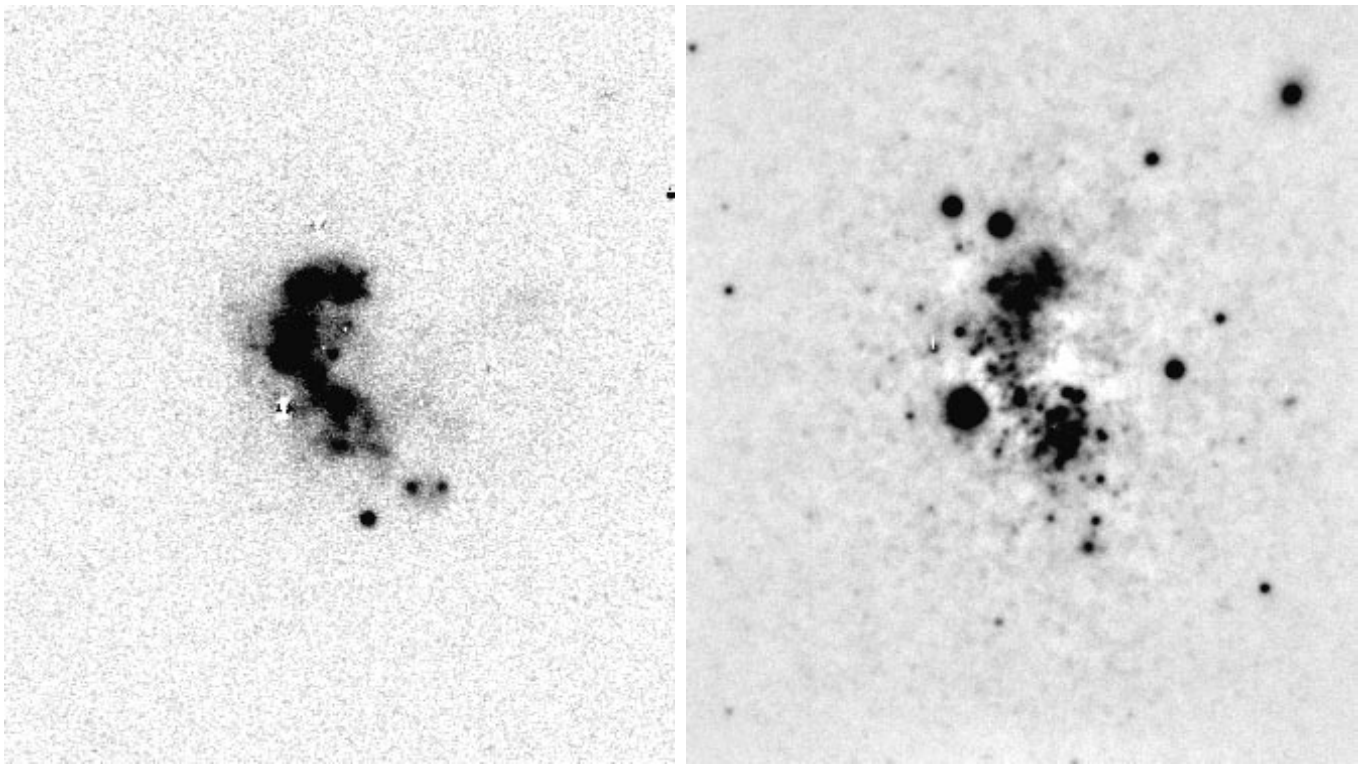

Fig. 2. Images of the central part of NGC 6789. **a)** An continuum-subtracted Hα image, **b)** the V band image after subtracting the median, smoothed with a window of $10 \times (FWHM)$. The total field is $1.22' \times 1.38'$. North left, East top

580 pixels, each 18×24 μm, and at the NOT the observations were carried out with Loral Lesser-thinned CCD chip having 2048 by 2048 pixels of 15 microns, that provided a $3'.7 \times 3'.7$ view field with a resolution of $0''.11$ per pixel. The journal of observations is given in Table 1. We used only the frames obtained under good photometric conditions with a seeing of $FMHM = 0''.7 - 1''.4$.

Table 1. Journal of observations

Telescope Date	Filter	Exposure (s)	Seeing (arcsec)
BTA 6 m	I	2×600	1.1
Apr. 23, 1996	R	600	1.4
BTA 6 m	I	600	0.9
Jul. 14, 1996	V	600	0.9
	B	600	0.9
Zeiss 1 m	B	2×600	1.1
Aug. 17, 1996	V	600	1.1
	R	600	1.1
	I	600	1.1
BTA 6 m	R	600	1.3
Jun. 14, 1997			
NOT 2.5 m	V	3×1000	0.7
Jul. 26, 1997	I	3×900	0.7
	Hα	2×1200	
	H$\alpha_{\rm Cont}$	2×1200	

After dark subtraction, flat-fielding and cleaning for cosmic events the photometric processing of the frames was performed with DAOPHOT and ALLSTAR packages (Stetson 1987) running within MIDAS. Equatorial photometric standards from Landolt (1992) were observed in all observing runs to transform instrumental magnitudes into the standard B, V, $R_{\rm c}$ & $I_{\rm c}$ system. The zero-point error does not exceed $0^{\rm m}.05$ for each spectral band.

Figure 1 shows the I image of NGC 6789 obtained with the NOT. For the analysis of stellar content, the observed field has been divided into several parts as indicated in the figure caption.

3. The results

3.1. Colour-magnitude diagram

The CM diagrams of regions C, E and F (see Fig. 1b) are shown in Fig. 3, where stars from region C are shown as open circles, stars from region E as filled diamonds and stars from the region F as dots.

The $[(V-I), I]$ CM diagram of the NGC 6789 shows characteristics typical of the CM diagrams of other dwarf galaxies, with evidence for both old and young populations. The main feature of the stars in the periphery of NGC 6789 CM diagram is the concentration that extends between $1^{\rm m}.2 \lesssim (V-I) \lesssim 2^{\rm m}.4$ and $I \gtrsim 21^{\rm m}.5$, which corresponds to RGB and asymptotic giant branch (AGB) old

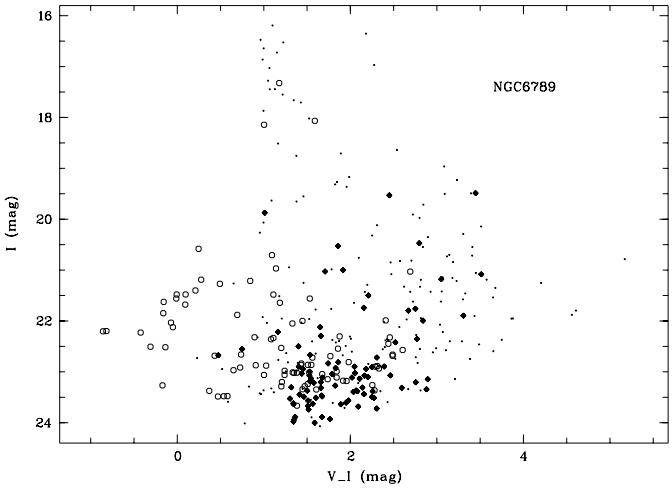

Fig. 3. Colour–Magnitude diagram for 337 stars in NGC 6789. The circles correspond to stars measured in the central region (C), the filled diamonds indicate stars in the periphery (E) and dots stars outside the galaxy (F)

and intermediate-age stars. There is also a considerable population of blue stars ($(V-I) \lesssim 0.7$) in the CM diagram of the central region. It is remarkable that these blue stars are entirely absent in the outer part of the galaxy. The presence of these stars in the central region, as well as the candidate H II regions in Hα image, shows that NGC 6789 is a BCD galaxy rather than a dE. Most of the bright stars ($I \lesssim 20^{\rm m}.5$) are likely foreground stars. According to our spectral long slit observations the brightest foreground star near the center of the galaxy is an F star.

The diagram shown in Fig. 3 has not been corrected for interstellar extinction. The galactic coordinates of NGC 6789 are $l_{\rm II} = 94^\circ.97, b_{\rm II} = 21^\circ.52$, and it lies in a region of moderate gradient with $E(B-V) = 0^{\rm m}.076$ in the extinction maps of Burstein & Heiles (1984). Using the extinction law of Cardelli et al. (1989) with $R_V = 3.3$, the extinction is: $A_B = 0^{\rm m}.32$, $A_V = 0^{\rm m}.24$, $A_R = 0^{\rm m}.21$ and $A_I = 0^{\rm m}.15$.

3.2. Metallicity

The average stellar metallicity can be obtained from the index $(V-I)_{-3.5}$, which is the colour index of the RGB half a magnitude below the tip of the RGB (TRGB) (see Da Costa & Armandroff 1990; Lee et al. 1993). We believe that the TRGB is at $I_{\rm TRGB} = 22^{\rm m}.7$ (see next section). The median colour between $I = 23^{\rm m}.4$ and $I = 24^{\rm m}.0$, that we take as $(V-I)_{-3.5}$, is $1^{\rm m}.7 \pm 0^{\rm m}.2$.

The corresponding dereddened value is $(V-I)_{-3.5,0} = 1^{\rm m}.6 \pm 0.2$. Using the calibration by Lee et al. (1993), we obtain a metallicity [Fe/H] $\simeq -1$ dex, and an internal abundance spread with total range of -0.8 dex is suggested by the intrinsic colour width of the RGB.

3.3. Distance

The absolute I magnitude of the TRGB gives a good estimate of distance (Lee et al. 1993). It is slightly dependent on the metallicity. To obtain the magnitude of the TRGB we have used the luminosity function (LF) of the stars in the colour interval $1\overset{\mathrm{m}}{.}0 < (V-I) \leq 3\overset{\mathrm{m}}{.}0$ for the external ring part of the galaxy (region E). Finally, an edge-detecting Sobel filter $[-1, 0, +1]$ (Sakai et al. 1996) has been applied to the LF. This produces a sharp peak at the TRGB corresponding to $I_{\mathrm{TRGB}} = 22\overset{\mathrm{m}}{.}7$. The resulting dereddened value is $I_{\mathrm{TRGB},0} = 22\overset{\mathrm{m}}{.}55$.

The colour of the TRGB is necessary to calculate the bolometric correction to be used in the I_{TRGB}-distance calibration. It is taken as the median colour index of the stars with $22\overset{\mathrm{m}}{.}7 \leq I \leq 22\overset{\mathrm{m}}{.}9$. We find $(V-I)_{\mathrm{TRGB}} = 1\overset{\mathrm{m}}{.}84$ which when corrected for external extinction yields $(V-I)_{\mathrm{TRGB},0} = 1\overset{\mathrm{m}}{.}75$. Using the calibration by Lee et al. (1993b), we obtain $M_{I,\mathrm{TRGB}} = -4\overset{\mathrm{m}}{.}10$.

We then derive a distance modulus $(m-M)_0 = 26\overset{\mathrm{m}}{.}65$, corresponding to 2.1 Mpc. The intrinsic error of the method is about $\pm 0\overset{\mathrm{m}}{.}1$ (see Lee et al. 1993). Our estimate of the stellar photometry errors is $\pm\ 0\overset{\mathrm{m}}{.}2$ due to severe crowding and high surface brightness in this galaxy. We adopt a total error of $0\overset{\mathrm{m}}{.}3$.

To see how near is NGC 6789 to the Local Group we construct a V_{helio} versus $\cos\Theta$ diagram (Fig. 4) for nearby galaxies closer than 2.5 Mpc, following the work of van den Bergh (1994) on the basis the data tabulated by Lee (1995), Karachentsev & Makarov (1996) and our own compilation. Θ is the angle between the center of the galaxy and the solar apex. We adopt a solar motion with respect to the Local Group members of 316 km s^{-1} toward the solar apex ($l_\odot = 93°, b_\odot = -4°$) given by Karachentsev & Makarov (1996). The crosses represent the satellites of the Milky Way Galaxy, the solid diamonds represent the satellites of M 31, the solid triangles are for members of the Sculptor group, and the open triangles are for members of the IC 342/Maffei complex. The open circles are galaxies not members of these subgroups. The envelope of the Local Group is represented by the dashed lines at ± 60 km s^{-1} from the central line with $V_\odot = -316\cos\Theta$ km s^{-1}.

We see that the NGC 6789 is probably not far from the Local Group. Note that NGC 6789 is a very isolated galaxy situated inside the Local Void described by Tully (1988).

3.4. Integrated light

Besides the stellar photometry we have performed the V, I and Hα surface photometry of the galaxy. We determined the surface brightness profiles in two steps. First, we calculated azimuthally averaged equivalent brightness profiles using the surface photometry routines developed at the Potsdam Astrophysical Institute. In this way we reduce the surface photometry to a one-dimensional profile. In addition to the differential radial surface brightness profiles we calculated the growth curve of the galaxy. The total magnitudes were estimated by asymptotic extrapolation of this growth curve.

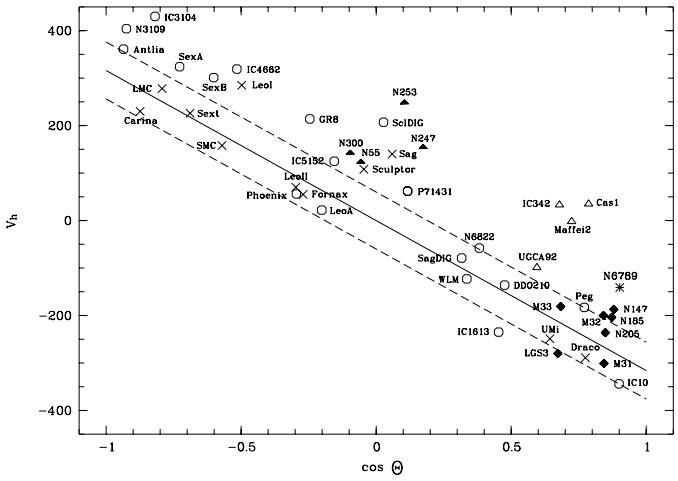

Fig. 4. Heliocentric velocity versus $\cos\Theta$ for nearby galaxies closer than 2.5 Mpc. Θ is the angle between the center of the galaxy and the solar apex. The crosses represent the satellites of the Milky Way Galaxy, the solid diamonds represent the satellites of M 31, the solid triangles are for members of the Sculptor group, and the open triangles are for members of the IC 342/Maffei complex. The open circles are for galaxies not members of these subgroups. The Local Group is defined as within the dashed lines at ± 60 km s^{-1} from the central line with $V_\odot = -316\cos\Theta$. The star represents the location of the NGC 6789

In order to obtain some information about the two-dimensional structure in a second round of calculations we used an ellipse fitting algorithm, which is based on the formulas given in Bender & Mölenhoff (1987) in its realization in the SURPHOT package running within MIDAS.

The resulting equivalent surface brightness distribution is shown in Fig. 5a. In both the V and I bands, the surface brightness distribution falls off as Gaussian from $\sim 5''$ to a radius of $\sim 20''$, and fairly flat from $\sim 20''$. The equivalent V band surface brightness can be well fitted by a Gaussian with a central surface brightness $\mu_0(V) = 21.7$ mag/$\Box''$ and a standard deviation $\sigma_V = 15.9''$ in the inner regions, and exponential profile with central surface brightness $\mu_0(V) = 21.8$ mag/$\Box''$ and exponential scale length $\alpha = 16.2''$ at larger radii. This gives an angular diameter at the $\mu_V = 26$ mag/$\Box''$ isophote of $\theta_{26} = 2.1'$; this corresponds to an isophote of $\mu_I = 25.0$ mag/$\Box''$. Given the distance of the galaxy, the break in the surface brightness profile occurs at $r_{\mathrm{equiv}} \approx 600$ pc.

Integrating the surface brightness profiles within the V and I bands out to the $\mu_V = 25$ mag/$\Box''$ isophote, we find $m_I = 13\overset{\mathrm{m}}{.}63\ \pm\ 0\overset{\mathrm{m}}{.}15$, and $m_V = 14\overset{\mathrm{m}}{.}62\ \pm\ 0\overset{\mathrm{m}}{.}15$, not

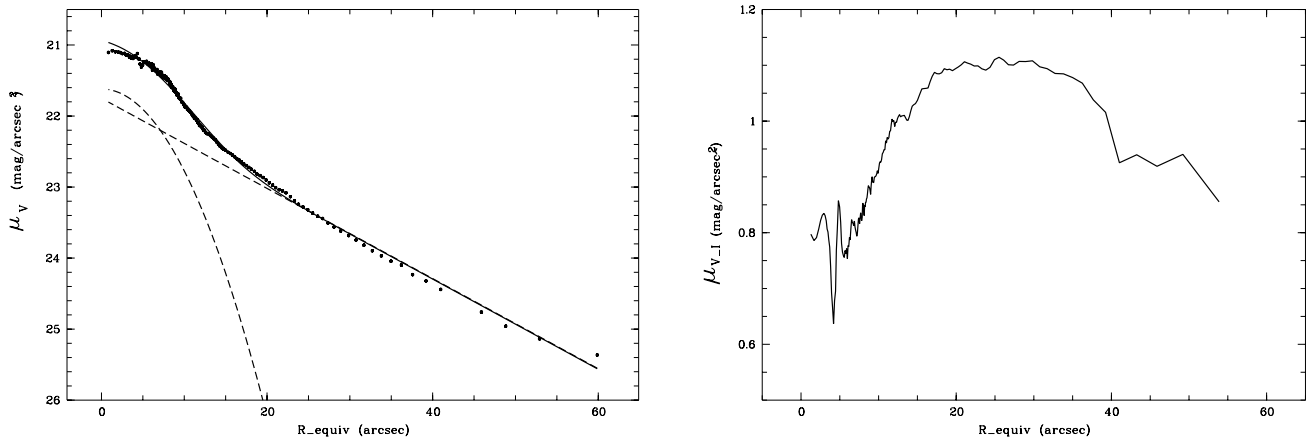

Fig. 5. Results of surface photometry of NGC 6789. **a)** Equivalent V surface brightness distribution. It can be fitted by an exponential law for the disk, and by a Gaussian law for the central region. The result of the fit is shown by the solid line. **b)** Surface colour $(V-I)$ profile

corrected for internal or galactic extinction. The quoted errors are an upper limit computed assuming that every point in Fig. 3 is systematically off by 1 σ. After correction for extinction (see Sect. 3.1) and considering the error in the distance modulus, the total absolute magnitude of NGC 6789 is $M_{I,0} = -13\overset{\mathrm{m}}{.}26 \pm 0\overset{\mathrm{m}}{.}35$ and $M_{V,0} = -12\overset{\mathrm{m}}{.}36 \pm 0\overset{\mathrm{m}}{.}35$. The integrated colour index $(V-I)_0$ increases smoothly from $0\overset{\mathrm{m}}{.}67$ in the center of NGC 6789 up to $0\overset{\mathrm{m}}{.}90$ within the largest visible radii (Fig. 5b). This is comparable to the colours of Scd & Im galaxies ($(V-I) = 0\overset{\mathrm{m}}{.}82$) for the Coleman et al. (1980) composite spectral energy distributions.

We also estimated a total Hα flux of NGC 6789, $F_{\mathrm{H}\alpha} \simeq 1.36\ 10^{-12}$ erg/(cm^2 s), after correction for galactic extinction. Since Hα-light comes from the gas excited by young hot stars, one can estimate a star formation rate on the basis of this line flux. Equation (1) is taken from the Hunter (1984):

$$SFR = 1.27\ 10^9 \cdot F_{\mathrm{H}_\alpha} \cdot D^2. \quad (1)$$

Here: SFR in $\mathcal{M}_\odot$/year units, F_{H_α} is the H$_\alpha$ flux corrected for interstellar extinction, in erg/(cm^2 s) units, D is the distance in the Mpc. Using our distance estimation we receive the full star formation rate in NGC 6789, $SFR \simeq 7.6\ 10^{-3}\mathcal{M}_\odot$/year, that is $\sim 3\ 10^{-8}\mathcal{M}_\odot$/year pc^2 on the part of area.

From the Hα luminosity it is possible to evaluate a number of young stars, whose light ionizes hydrogen in a galaxy. The number of Layman continuum quants (Ly-c), radiated by galaxy stars in one second is

$$\mathcal{N}_{\mathrm{Ly-c}} = 7.43\ 10^{11}\ L_{\mathrm{H}\alpha}. \quad (2)$$

The galaxy luminosity in Hα, $L_{\mathrm{H}\alpha}$, is calculated from the flux and galaxy distance. This equation is taken from the work of Mass-Hess & Kunth (1991). Taking into account that one O7 V type star emits $\sim 10^{49}$ Ly-c quants per second we obtain an approximate number of such stars in NGC 6789, $\mathcal{N}_{\mathrm{Ly-c}} \simeq 50$. We have successfully resolved about twenty brightest blue stars in the central part of this galaxy. The most part of these stars hides in the compact star formation regions.

4. Concluding remarks

We have presented the B, V, R, I photometry of 337 resolved stars in the blue compact dwarf galaxy NGC 6789. The CM diagram shows two stellar populations distinct in structure and colour: an underlying older low-surface-brightness stellar population formed previously to the present burst, and an inner high-surface-brightness young population within 150 pc from the center of the galaxy.

The tip of the first ascent RGB is used to estimate a metallicity ([Fe/H] ~ -1 dex) and distance of the NGC 6789 (about 2.1 Mpc).

NGC 6789 has a light distribution which is well described by combination of the Gaussian and exponential laws. Its central surface brightness is $\mu_0(V) = 21.1$ mag/$\square''$, and its isophotal equivalent diameter is $\theta_{26,\mathrm{equiv}} = 2\farcm1$ or $D_{26,\mathrm{equiv}} = 1.2$ kpc, making it an intrinsically small high surface brightness galaxy. NGC 6789's integrated absolute magnitude within $\mu_V = 25$ mag/$\square''$ is $M_{V,0} = -12\overset{\mathrm{m}}{.}36 \pm 0\overset{\mathrm{m}}{.}35$. It is also quite blue: $((V-I) = 0\overset{\mathrm{m}}{.}67)$ in its central region, but its halo much redder, so the total colour index of NGC 6789 inside the $\mu_V = 25$ mag/$\square''$ isophote is $(V-I) = 0\overset{\mathrm{m}}{.}90$.

The total Hα flux of NGC 6789 is $F_{\mathrm{H}\alpha} \simeq 1.36\ 10^{-12}$ erg/(cm^2 s). A corresponding current star formation rate, $SFR \simeq 7.6\ 10^{-3}\mathcal{M}_\odot$/year. To account for the observed radiation of the ionized gas it is necessary about 50 O7 V stars. Such a high star formation rate could not be constant during the long time due to absence gas supply supporting this process (let us remind that HI flux was undetected which indicates an absence of large gas stock). After $\sim 10^6$ years this galaxy should turn to the another evolution phase.

Recent observations have shown that the division of dwarf galaxies into irregulars (dIrs) and ellipticals (dEs + dSphs) is often quite ambiguous. Dwarf galaxies vary widely in shape and properties and call to a revision of our current understanding of their nature and evolution.

In accordance to this results we can conclude that NGC 6789 belongs to the group of blue compact dwarf (BCD) galaxies, which have an irregular patchy blue central part with large H II regions and bright blue stars. They show no prominent nucleus while their outer regions have a smooth spheroidal shape and an old red stellar population, as dwarf ellipticals. According to the classification scheme of Loose & Thuan (1985), NGC 6789 may be classified of the "iE" type, comprising $\sim$70% of BCD, which combines irregular inner isophotes with accurately elliptical outer isophotes. The intensive star formation observed in the central region of NGC 6789 contrasts with the absence of the significant young population in the outer regions and suggests a two-component (core-halo or disk-halo) structure of the galaxy. This seems to be common not only in large spirals but also in dwarfs (see for example the case of WLM; Minniti & Zijstra 1996, and Antlia; Aparicio et al. 1998). The nearby galaxies GR 8 (Tikhonov & Drozdovsky 1998b), NGC 4163 (Tikhonov & Karachentsev 1998a), NGC 1705 (Meurer et al. 1992), NGC 2915 (Meurer et al. 1996), and UGC 1104 (Sharina et al. 1996) are probably the most similar to NGC 6789.

The detection of an extended faint stellar underlying component (Loose & Thuan 1985, 1986; Kunth et al. 1988), in the majority of BCDs supports the idea that they are not truly primordial galaxies, but older LSB dwarf galaxies undergoing transient periods of star formation. In the case of NGC 6789 a continuous gas infall from the halo and its accumulation in the central part could lead to the present burst of the star formation. All accumulated gas proved to be involved in this burst. This can explain the present picture: a presence of rather large amounts of the ionized hydrogen in the central region of the galaxy despite of the lack of detected H I gas.

Acknowledgements. We are grateful to Dr. A. Aparicio for his participation in the observations with NOT and basic CCD frames reduction from this run. This work is partially supported by RFBR grant No. 97-02-17163 and INTAS-RFBR grant No. 95-IN-RU-1390. ID thanks the Special Astrophysical Observatory for its hospitality. Dr. Lequeux comments and corrections to the previous version of this paper were of invaluable help. This research has made use of the NASA/IPAC extragalactic database (NED) which is operated by the Jet Propulsion Laboratory, Caltech, under contract with the National Aeronautics and Space Administration.

References

Aparicio A., Dalcanton J.J., Gallart C., Martinez-Delgado D., 1997, AJ 114, 1447
Burstein D., Heiles C., 1984, ApJS 54, 33
Bender R., Möllenhoff C., 1987, A&A 177, 71
Cardelli J.A., Clayton G.C., Mathis J.S., 1989, ApJ 345, 245
Coleman C.D., Wu C.-C., Weedman D.W., 1980, ApJS 43, 393
Da Costa G.S., Armandroff T.E., 1990, AJ 100, 162
de Vaucouleurs G., de Vaucouleurs A., Corwin H.G., Buta R.J., Paturel G., Fouque P., 1991, Third reference Catalog of Bright Galaxies. New York: Springer-Verlag
Huchra J.P., Geller M.J., Clemens C.M., Tokarz S.P., Michel A., 1995, The CfA Redshift Catalogue, NSSDC/ADC Cat. A 7193. Greenbelt, MD: GSFC
Huchtmeier W.K., Karachentsev I.D., Karachentseva V.E., 1997, A&A 322, 375
Hunter D.A., 1984, ApJ 284, 544
Karachentsev I.D., Makarov D.I., 1996, AJ 111, 794
Karachentsev I.D., Makarov D.I., 1998, A&A 331, 891
Karachentseva V.E., Karachentsev I.D., 1998, A&AS 127, 409
Kunth D., Maurogordato S., Vigroux L., 1988, A&A 204, 10
Landolt A.U., 1992, AJ 104, 340
Lee M.G., Freedman W.L., Madore B.F., 1993, ApJ 417, 553
Lee M.G., 1995, JKAS 28, 169
Loose H.H., Thuan T.X., 1985, in Star-Forming Dwarf Galaxies and Related Objects, Kunth D., Thuan T.X., & Van T.T. (eds.). Paris: Éditions Frontières, p. 73
Loose H.H., Thuan T.X., 1986, ApJ 309, 59
Mass-Hess J.M., Kunth D., 1991, A&AS 88, 399
Meurer G.R., Freeman K.C., Dopita M.A., Cacciari C., 1992, AJ 103, 60
Meurer G.R., Carignan C., Beaulieu S.F., Freeman K.C., 1996, AJ 111, 1551
Minniti D., Zijstra A.A., 1996, ApJ 463, L13
Papaderos P., Loose H.-M., Fricke K.J., Thuan T.X., 1996, A&A 314, 59
Sakai S., Madore B.F., Freedman W.L., 1996, ApJ 461, 713
Sharina M.E., Karachentsev I.D., Tikhonov N.A., 1996, A&AS 119, 499
Stetson P.B., 1987, PASP 99, 191
Tikhonov N.A., Karachentsev I.D., 1998, A&AS 128, 325
Tikhonov N.A., Drozdovsky I.O., 1998 (in preparation)
Tully R.B., 1988, Nearby Galaxies Catalogue. Cambridge, Cambridge Univ. Press
van den Bergh S., 1994, AJ 107, 1328